

Available online at www.sciencedirect.com

ScienceDirect





Original Article

Neuroprotective effect of tanshinone IIA against neuropathic pain in diabetic rats through the Nrf2/ARE and $NF-\kappa B$ signaling pathways



Fa-Bo Feng a, Hai-Yan Qiu b,*

Received 16 November 2017; accepted 7 March 2018 Available online 27 April 2018

KEYWORDS

Nrf2/ARE signaling pathway; NF-kB signaling pathway; Tanshinone IIA; Diabetic rats; Neuropathic pain Abstract The study aims to investigate whether tanshinone (TSN) IIA affects diabetic neuropathic pain (DNP) via the Nrf2/AR and NF-κB signaling pathways. Rats were randomly assigned into DNP group, TSN group (injected with TSN IIA), TSN + DRB group (injected with TSN IIA and 15 mg/kg Nrf2/ARE inhibitors), TSN + PDTC group (injected with TSN IIA and 60 mg/kg NF- κ B inhibitors) or control group. The first four groups were successfully established as DNP models after injection of streptozotocin. The blood glucose level, mechanical withdrawal threshold (MWT), thermal withdrawal latency (TWL), nerve conduction velocity (NCV) and antioxidase level were detected. Transmission electron microscopy and toluidine blue staining were utilized to observe the sciatic nerve. RT-qPCR and western blot were used to measure expression levels of Nrf2/ARE and NF-κB signaling pathway-related genes. Blood glucose, malondialdehyde (MDA) and erythrocyte glutathione peroxidase (GSH-Px) levels as well as expression of Keap1 and NF- κ B were increased in the TSN, TSN + DRB and TSN + PDTC groups compared to control group. Furthermore, the MWT, TWL, NVC, and superoxide dismutase (SOD) levels and expression of Nrf2, heme oxygenase 1 (HO-1) and inhibitory kappa B (lκB) decreased in the treatment groups. The TSN + DRB and TSN + PDTC groups showed similar trend when compared with the TSN group, while the opposite trend was observed in the TSN group when compared with the DNP group. Our study demonstrates that TSN IIA alleviates neuropathic pain by activating the Nrf2/ARE signaling pathway and inhibiting the NF-κB signaling pathway in dia-

Copyright © 2018, Kaohsiung Medical University. Published by Elsevier Taiwan LLC. This is an open access article under the CC BY-NC-ND license (http://creativecommons.org/licenses/by-nc-nd/4.0/).

E-mail address: qiuhaiyanbecky@126.com (H.-Y. Qiu).

^a Department of Orthopedics, Zhejiang Provincial People's Hospital, People's Hospital of Hangzhou Medical College, Hangzhou, PR China

^b Department of Endocrinology, Hangzhou First People's Hospital, Nanjing Medical University, Hangzhou, PR China

Conflicts of interest: All authors declare no conflicts of interests.

^{*} Corresponding author. Department of Endocrinology, Hangzhou First People's Hospital, Nanjing Medical University, No. 261, Huansha Road, Hangzhou 310006, Zhejiang Province, PR China.

Introduction

After nerve injury, neuropathic pain can occur when there are deleterious changes in injured neurons through pathways with nociception and descending modulation in the central nervous system [1]. A variety of diseases or injuries have been reported to be responsible for neuropathic pain, including diabetes [2]. One of the most typical complications in diabetic patients is neuropathic pain that results from a lesion or somatosensory system-related disease [3]. Diabetic neuropathic pain (DNP), a class of nerve disorders including peripheral, autonomic, proximal and focal aspects, occurs in approximately 10-20% of patients with diabetes and occurs in approximately 40-50% of patients with diabetic neuropathy [4,5]. Burning, tingling, shooting and/or lancing are representative symptoms of DNP [6]. Neuropathic pain is a clinical symptom that poses special diagnostic and therapeutic challenges [7]. Although it is well-known that pain is one of the major characteristics of diabetic neuropathy, the underlying pathophysiological mechanisms are not yet clearly understood [8]. Hence, more studies are needed to further develop novel mechanism-based therapeutic agents.

Tanshinone IIA (TSN IIA) is one of the most active components of the traditional Chinese herbal medicine Danshen, which is popularly used in the treatment of cerebrovascular and cardiovascular diseases in China [9]. In Asian countries, the safety of TSN IIA treatment has been well-established, and it is widely used for the treatment of arrhythmia, acute ischemic stroke and angina pectoris [10]. Recently, it has been recognized that TSN IIA plays a critical role in alleviation of inflammatory and neuropathic pain by inhibiting HMGB1 expression [11]. Moreover, TSN IIA has been reported to induce nuclear factor (erythroid-derived 2)-like 2 (Nrf2) activation, which is a major regulatory pathway of cytoprotective gene expression against oxidative stress [12]. Nrf2 regulates a number of antioxidant response element (ARE)-regulated genes [13]. AREs are cis-acting components that regulate many phase 2 genes, encoding proteins that prevent oxidative and electrophilic stresses [14]. The Nrf2/ARE signaling pathway is an endogenous and ubiquitously expressed cytoprotective system, and the transcription factor Nrf2 is a basic leucine zipper protein of the system that regulates the expression of antioxidant proteins [15]. Nuclear factor-kappa B (NF-κB) is a protein associated with diverse physiological and pathological processes [16]. NF-κB is widely distributed, regulates the expression of multiple important genes and is involved in innate immunity, inflammation and a number of cellular processes, such as cell proliferation, transformation and apoptosis [17]. TSN IIA can inhibit NF-kB and AP-1 DNA-binding, which inhibits the migration of human aortic smooth muscle cells [18]. Recently, NF-κB has been confirmed to mainly modulate pro- and anti-nociceptive factors of neuropathic pain [19]. Therefore, the role of TSN IIA in DNP via the Nrf2/ARE and NF-kB signaling pathways is investigated in this study.

Materials and methods

Ethics statement

The animal experimental processes were approved by the Ethics Committee of our hospital and conducted in strict accordance with the standards of animal protection, animal welfare and ethical principles of the Institutional Animal Care and Use Committee (IACUC) (IACUC approval number: 201709003).

Model establishment and animal grouping

A total of 160 male clean-grade (without any specific pathogen or parasite that may affect the experiment) Sprague-Dawley (SD) rats (weighing 220-250 g) were purchased from the Experimental Animal Center of the Chinese Academy of Sciences (Shanghai, China). The rats were housed at 20-25 °C with an alternating 12 h light-dark cycle and had free access to water and food for 72 h. Rat models of DNP were established [20]. Streptozotocin (STZ, K0050, Shanghai Kexing Biotechnology Co., Ltd., Shanghai, China) was injected intraperitoneally at a dose of 75 mg/kg after fasting for 12-16 h (with free water). Three days after injection, diabetes was confirmed by blood sample collection through the tail vein. Blood glucose concentrations over 16.7 mmol/l implied type I diabetes, and a mechanical withdrawal threshold (MWT) level less than 15 g indicated the successful establishment of rat models with DNP. The rats with successful model establishment were randomly divided into 4 groups, with 32 rats in each group: a DNP group, a TSN IIA (TSN) group, a TSN + DRB group and a TSN + PDTC group. Another 32 normal rats were enrolled in the control group. The rats in the control and DNP groups were fed a normal diet without any treatment. The rats in the TSN, TSN + DRB and TSN + PDTC groups were intraperitoneally injected with TSN IIA (CP-111605, Shanghai Yubo Biotechnology Co., Ltd., Shanghai, China) at a dose of 25 mg/kg once per day for 28 days. The rats in the TSN + DRB and TSN + PDTC groups were intravenously injected with Nrf2/ARE5 inhibitor 5,6dichlorobenzimidazole1-β-p-ribofuranoside (DRB) (15 mg/ kg, 10010302, Beijing Biopike Biotechnology Co., Ltd., Beijing, China) and NF-κB inhibitor pyrrolidine dithiocarbamate (PDTC), (60 mg/kg, 1676-100, Shanghai Lanjun Biotechnology Co., Ltd., Shanghai, China), respectively, once per day for 28 days. The rats were sacrificed 28 days after injection, and 8 rats were randomly selected from each group 1 h before model establishment (T1), 1 h after model establishment (T2), and on the 2nd weekend (T3) and the 4th weekend (T4) after injection.

Blood glucose test

Blood glucose was tested at different time points (T1, T2, T3 and T4). The rats were fasted for 6–7 h and anesthetized with ether, and blood was obtained from the eye plexus. Then, the blood was clotted at room temperature for 60 min

and centrifuged at $1000 \times g$ for 20 min to separate serum. Glucose concentration was then determined using the glucose oxidase method. According to the instructions of the Glucose Reagent Kit (D107, Beijing Solarbio Science & Technology Co., Ltd., Beijing, China), the absorbance was measured using an ultraviolet—visible spectrophotometer (α 1900S, Shanghai Puyuan Instruments Co., Ltd., Shanghai, China) at 505 nm and expressed as mmol/l.

Behavioral test

MWT was measured for mechanical allodynia. The rats were placed in a transparent plexiglass box with a 1 cm \times 1 cm wire mesh at the bottom and acclimated for 15 min. An electronic pressure sensor (Φ 0.5 mm probe) was used to stimulate the plantar surface of the left hind paw. Paw lifting or licking was interpreted as a positive response, except which the response was negative. Values on the screen were recorded (unit: g) at 30-s intervals, and the tests were performed 3 times forin both the left and right paws. Since there were fluctuations in the first recorded values, only the mean values of the last five recordings were included in this study.

Thermal withdrawal latency (TWL) was measured for thermal hyperalgesia. The rats were placed in a plexiglass box (3 mm in thickness, 22 cm \times 12 cm \times 22 cm) and acclimated for 15 min. The center of the hind paw was exposed to a halogen lamp. The parameters of the thermal radiation stimulator (BIO-TGT2, Bioseb, Chaville, France) were set at 20% radiant heat without measurement, 60% radiant heat during measurement, a cut-off time of 25 s to prevent damage to rats, and a starting temperature of 30 °C. The reaction time started from the beginning of radiation treatment until the rat lifted its hind paw and was recorded as the TWL. The measurement was alternately repeated 3 times at 5-min intervals between the right and left hind paw. Since there were fluctuations in the first recorded values, only the mean values of the last five recordings were included in this study.

Nerve conduction velocity (NCV) test

The NCV was detected by electromyogram (EMG) (Dantec Cantata, Copenhagen, Denmark). The rats were anesthetized by intraperitoneal injection of 1% sodium pentobarbital solution at a dose of 40 mg/kg (P3761, Sigma, St Louis, MO, USA) for exposure of the left sciatica nerve. The stimulating electrode was inserted into the sciatic nerve, and the leading electrode was inserted into the gastrocnemius. After the stimulating electrode discharged, the conduction time (latency of compound action potential) was recorded. The distance between the stimulating electrode and the leading electrode along the sciatic nerve was measured. NCV was calculated using the formula NCV (m/s) = distance/conduction time.

Transmission electron microscopy (TEM)

Rats were sacrificed 28 d after injection, and a skin incision was made between the right bicep and the semi-membranosus. Blunt separation was conducted to expose

the sciatic nerve. The surgical scissor was used to obtain the left sciatic nerve (1.0–2.0 cm) from the rats with DNP. The sciatic nerve was fixed with 25 g/l glutaraldehyde and 10 g/l osmic acid, dehydrated with gradient ethanol and acetone, soaked with acetone and embedding solution and heated at 37 °C, 45 °C and 60 °C. The specimens were sectioned into 55–60 nm slices with a microtome (TCH-CP20, Shenzhen Teensky Technology Co., Ltd., Shenzhen, China), stained with uranyl acetate and lead citrate, observed and photographed under a scanning electron microscope (SU1510, Hitachi Ltd., Tokyo, Japan).

Toluidine blue staining

The surgical scissor was used to obtain the right sciatic nerve (1.0 cm from the sciatica nerve). The sciatic nerve was fixed with the same fixation liquid for 48 h and washed with phosphate buffer solution (PBS). The specimens were fixed again with osmic acid, dehydrated with ethanol, embedded in Epon, cut into semi-thin sections (1 μ m) and stained with toluidine blue. Metamorph (NIC, USA)/DP10/Bx51 (Olympus, Japan) was used to analyze the image.

Coomassie brilliant blue staining

Part of the sciatic nerve was added to a 0.9% sodium chloride solution to make a 5% homogenate, which was centrifuged at 350 \times g for 10 min. The supernatant was obtained and diluted with 0.9% sodium chloride solution (1:1) to make a 2.5% homogenate. According to the manufacturer's instructions, a xanthine oxidase method (SD103, Shanghai Solarbio Science & Technology Co., Ltd, Shanghai, China), a 5,5'-dithiobis (2-nitrobenzoic acid) (DTNB) method (QS1202, Shanghai Solarbio Science & Technology Co., Ltd, Shanghai, China) and a thiobarbituric acid (TBA) (SD105, Shanghai Solarbio Science & Technology Co., Ltd, Shanghai, China) method were used to detect superoxide dismutase (SOD), erythrocyte glutathione peroxidase (GSH-Px) and malondialdehyde (MDA), respectively. The antioxidase activity in the sciatic nerve was determined using Coomassie brilliant blue staining.

Reverse transcription quantitative polymerase chain reaction (RT-qPCR)

Total RNA was extracted using Trizol reagent (15596-018, Invitrogen, Carlsbad, CA, USA) according to the manufacturer's instructions. Ultrapure water was used to dissolve RNA, and an ultraviolet-visible spectrophotometer (ND-1000, ThermoScientific, MA, USA) was used to measure the absorbances at 260 and 280 nm to detect the quality of total RNA. Then, the RNA concentration was adjusted. Reverse transcription of RNA was conducted according to the manufacturer's instructions (ThermoScientific, MA, USA). The reaction conditions of reverse transcription were 70 °C for 10 min, ice bath for 2 min, 42 °C for 60 min and 70 °C for 10 min. The cDNA was stored at -80 °C. RT-qPCR was performed according to the manufacturer's instructions (ThermoScientific, MA, USA) using a PCR instrument (Bio-Rad iQ5, Bio-Rad, San Francisco, USA). The primers were designed according to the GenBank database and then

Table 1	Primer sequences for RT-qPCR.	
Genes	Forward primers (5'-3')	Reverse primers (5'-3')
Keap1	TGCAAATGGATTCTGCTTCACCTACTTTGCAGGAA	TGAGCCCAGAACCTCCTTTTTCTCCAGTTTC
Nrf2	GCAACTCCAGAAGGAACAGG	GGAATGTCTCTGCCAAAAGC
HO-1	CTTTCAGAAGGGTCAGGTGTC	TGCTTGTTTCGCTCTATCTCC
NF-κB	CATGCGTTTCCGTTACAAGTGCGA	TGGGTGCGTCTTAGTGGTATCTGT
IκB	TGG CCA GTG TAG CAG TCT TG	GAC ATC AGC ACC CAA AGT CA
GAPDH	TATGACAACTCCCTCAAGAT	GGCATGGACTGTGGTCATGA

Note: glyceraldehyde-3-phosphate dehydrogenase; Nrf2, nuclear factor (erythroid-derived 2)-like 2; NF- κ B, nuclear factor-kappa B; HO-1, heme oxygenase 1; I κ B, inhibitory kappa B; RT-qPCR, reverse transcription quantitative polymerase chain reaction.

synthesized. The primer sequences are shown in Table 1. The reaction system included 12.5 μ l Premix Ex Taq or SYBR Green Mix, 1 μ l forward primer, 1 μ l reverse primer, and 1–4 μ l DNA template, and the reaction was brought to 25 μ l with double distilled water (ddH2O). The conditions were pre-denaturation at 95 °C for 30 s, 40 cycles of denaturation at 95 °C for 10 s, annealing at 60 °C for 20 s and extension at 70 °C for 10 s. Glyceraldehyde-3-phosphate dehydrogenase (GAPDH) was used as an internal reference, and the 2- $\Delta\Delta$ CT method was used to calculate the relative expressions of target genes. The 2- $\Delta\Delta$ Ct is the ratios of the target gene expression in the experiment and control groups. The formulas were as follows: $\Delta\Delta$ CT = Δ Ct experiment group – Δ Ct control group, Δ Ct = Ct target gene – Ct GADPH. The experiment was repeated 5 times.

Western blot analysis

The sciatic nerve was quickly removed, ground with liquid nitrogen, transferred to a 5 ml centrifuge tube and combined with 100 μ l RIPA lysis buffer containing 1 mmol/l PMSF (R0020, Beijing Solarbio Science & Technology Co., Ltd., Beijing, China). After centrifugation at 350 \times g, the sample was placed on ice at 4 °C for 30 min and centrifuged at $12,000 \times g$ for 4 min. The supernatant was collected and stored at -80 °C. The protein concentration was determined using the BCA Protein Assay Kit (AR0146, Wuhan Boster Biological Technology, Wuhan, China) and adjusted to 3 μg/μl. The extracted proteins (30 μg/well) were mixed with a loading buffer, boiled at 95 °C for 10 min, and separated by 10% polyacrylamide gel (Wuhan Boster Biological Technology, Wuhan, China). After electrophoresis, the proteins were transferred to a polyvinylidene fluoride (PVDF) membrane (P2438, Sigma, St Louis, MO, USA). The membrane was blocked with 5% bovine serum albumin (BSA) for 1 h and then incubated with the following primary antibodies (all rabbit antibodies) overnight at 4 °C: Keap1 (1: 1000, ab196346, Abcam, Inc., MA, USA), Nrf2 (1: 2000, ab62352, Abcam, Inc., MA, USA), heme oxygenase-1 (HO-1) (1: 2000, ab52947, Abcam, Inc., MA, USA), NF-κB (1: 1000, ab32360, Abcam, Inc., MA, USA) and inhibitory kappa B (IkB) (1: 500, ab64813, Abcam, Inc., MA, USA). After washing with Tris-buffered saline with Tween 20 (TBST) three times (5 min each), the membrane was incubated with rabbit secondary antibody (ab150077, Abcam, Inc., MA, USA) for 1 h and then washed with TBST three times (5 min each). The proteins were detected by chemiluminescence reagent (NCI 5080, Shanghai Yanhui Biotechnology Co., Ltd., Shanghai, China), and images were obtained using the Gel Doc EZ system (Bio-Rad, California, USA). GAPDH was used as an internal reference. The gray values of target protein bands were analyzed using ImageJ software.

Statistical analysis

The SPSS 21.0 software (IBM Corp, Armonk, NY, USA) was adopted for statistical analysis. All measurement data were expressed as the mean \pm standard deviation. A normality distribution test of the data was analyzed using the D'Agostino & Pearson omnibus normality test. When data were normally distributed, the comparisons among the multiple groups were performed using one-way analysis of variance, and the comparisons between two groups were analyzed using Tukey's post hoc test. Dunn's multiple comparison post hoc test, a variation of the Kruskal–Wallis test, was conducted for analysis of data that were not normally distributed. p < 0.05 was considered to be statistically significant.

Results

Blood glucose levels at different time points in the control, DNP, TSN, TSN + DRB and TSN + PDTC groups

The blood glucose levels of each group are shown in Table 2. There was no significant difference in blood glucose levels in the control group at each time point (all p > 0.05). However, blood glucose levels in the DNP, TSN, TSN + DRB and TSN + PDTC groups significantly increased after injection of STZ (all p < 0.05). Additionally, the blood glucose levels in the DNP, TSN + DRB and TSN + PDTC groups were higher at T3-T4, while the blood glucose levels in the TSN group significantly declined over time (Post hoc: control vs DNP, p = 0.001; control vs TSN, p = 0.001; control vs TSN + DRB, p = 0.001; control vs TSN + PDTC, p = 0.001). Compared with the control group, the blood glucose levels in the DNP, TSN, TSN + DRB and TSN + PDTC groups increased significantly after model establishment (all p < 0.05). Compared with the DNP group, the blood glucose level in the TSN group significantly decreased (Post hoc: control vs DNP, p = 0.001). The blood glucose levels in the TSN + DRB and TSN + PDTC groups were notably higher

Table 2 The blood glucose levels at different time points (mmol/L).					
Group	T1	T2	T3	T4	
Control (n = 8)	$\textbf{5.62} \pm \textbf{0.23}$	$\textbf{5.70} \pm \textbf{0.43}$	5.49 ± 0.45	5.59 ± 0.40	
DNP $(n = 8)$	$\textbf{5.65} \pm \textbf{0.33}$	26.84 \pm 1.78*%	26.92 \pm 1.87*%	26.11 \pm 1.66*%	
TSN (n = 8)	5.59 ± 0.35	26.93 \pm 1.78*%	19.96 \pm 0.99*#%&	15.67 \pm 0.60*#%&\$	
TSN + DRB (n = 8)	$\textbf{5.66}\pm\textbf{0.50}$	26.98 \pm 1.98*%	26.95 \pm 1.91*%	26.94 \pm 1.86*%	
TSN + PDTC (n = 8)	$\textbf{5.69} \pm \textbf{0.43}$	26.89 \pm 2.01*%	$\textbf{26.87}\pm\textbf{1.69*\%}$	$\textbf{26.94}\pm\textbf{1.88*\%}$	

Note: *, p < 0.05 compared with the control group at the same time point; $^{\#}$, p < 0.05 compared with the DNP group at the same time point; $^{\$}$, p < 0.05 compared with the time point of T1; $^{\$}$, p < 0.05 compared with the time point of T2; $^{\$}$, p < 0.05 compared with the time point of T3; T1, 1 h before model establishment; T2, 1 h after model establishment; T3, on the 2nd weekend after injection; T4, on the 4th weekend after injection; DNP, diabetic neuropathic pain; TSN, tanshinone IIA; DRB, 5, 6-dichlorobenzimidazole1- β -p-ribofuranoside; PDTC, pyrrolidine dithiocarbamate.

than those in the TSN group (all p < 0.05), and there were no significant differences among the DNP, TSN + DRB and TSN + PDTC groups at any time point (all p > 0.05).

Mechanical allodynia and thermal hyperalgesia at different time points in the control, DNP, TSN, TSN + DRB and TSN + PDTC groups

The MWT and TWL values are shown in Table 3. No significant differences in MWT and TWL were observed in the control group (all p > 0.05). Compared with the groups before model establishment, the DNP, TSN, TSN + DRB and TSN + PDTC groups exhibited a significant decrease in the MWT and TWL (all p < 0.05). The MWT and TWL in the DNP, TSN + DRB and TSN + PDTC groups remained at a low level at T3-T4, while the levels in the TSN group significantly increased at T3-T4 (all p < 0.05). Compared with the control group, the MWT and TWL in the DNP, TSN, TSN + DRB and TSN + PDTC groups significantly decreased (all p < 0.05). Compared with the DNP group, the MWT and TWL in the TSN group significantly increased (all p < 0.05). Notably, the MWT and TWL in the TSN + DRB and TSN + PDTC groups were lower than those in the TSN group (all p < 0.05), and there were no significant differences in the MWT and TWL among the DNP, TSN + DRB and TSN + PDTC groups at any time point (all p > 0.05).

NCV at different time points in the control, DNP, TSN, TSN + DRB and TSN + PDTC groups

The NCV is shown in Table 4. There were no significant differences in NCV in the control group (all p > 0.05). Compared with each group before model establishment, the NCV in the DNP, TSN, TSN + DRB and TSN + PDTC groups was significantly decreased (all p < 0.05). The NCV in the DNP, TSN + DRB and TSN + PDTC groups was low at T3-T4, while the NCV in the TSN group was significantly increased (all p < 0.05). Compared with the control group, the NCV in the DNP, TSN, TSN + DRB and TSN + PDTC groups significantly decreased after model establishment (all p < 0.05). Compared with the DNP group, the NCV in the TSN group significantly increased (all p < 0.05). Compared with the TSN group, the NCV in the TSN + DRB and TSN + PDTC groups significantly decreased (all p < 0.05). However, there were no significant differences in the NCV among the DNP, TSN + DRB and TSN + PDTC groups at any time point (all p > 0.05).

Table 3 MWT and TWL at different time points in five groups.					
Parameters	Group	T1	T2	T3	T4
MWT (g)	Control (n = 8)	43.00 ± 2.90	43.21 ± 3.51	45.13 ± 4.21	44.78 ± 5.12
	DNP $(n = 8)$	43.63 ± 3.11	21.73 \pm 1.03*%	20.84 \pm 0.99*%	19.36 \pm 0.87*%
	TSN (n = 8)	$\textbf{43.75}\pm\textbf{3.42}$	21.18 \pm 1.12*%	$28.23\pm2.01*$ #%&	$35.61 \pm 3.28*#\%$ &\$
	TSN + DRB (n = 8)	43.87 ± 5.12	21.86 \pm 2.23*%	22.88 \pm 2.01*%	20.52 \pm 1.69*%
	TSN + PDTC (n = 8)	43.12 ± 3.21	21.29 \pm 2.11*%	20.33 \pm 1.95*%	20.01 \pm 0.99*%
TWL (s)	Control $(n = 8)$	16.10 ± 1.70	$\textbf{16.50} \pm \textbf{1.63}$	16.19 ± 1.74	$\textbf{16.09}\pm\textbf{2.01}$
	DNP $(n = 8)$	16.04 ± 1.31	8.73 \pm 0.78*%	$\textbf{8.74}\pm\textbf{0.69*\%}$	8.64 \pm 0.83*%
	TSN (n = 8)	$\textbf{16.02}\pm\textbf{0.71}$	9.00 \pm 0.54*%	10.52 \pm 1.01*#%&	$13.14 \pm 1.01*$ #%&\$
	TSN + DRB (n = 8)	$\textbf{16.06}\pm\textbf{1.41}$	8.84 \pm 0.88*%	$\textbf{8.59}\pm\textbf{0.49*\%}$	8.61 \pm 0.73*%
	TSN + PDTC (n = 8)	16.11 ± 1.39	$\textbf{8.64} \pm \textbf{0.68*}\%$	$\textbf{8.65}\pm\textbf{0.49*\%}$	8.51 \pm 0.81*%

Note: * , p < 0.05 compared with the control group at the same time point; * , p < 0.05 compared with the DNP group at the same time point; * , p < 0.05 compared with the time point of T1; $^{\hat{\mathbf{u}}}$, p < 0.05 compared with the time point of T2; 5 , p < 0.05 compared with the time point of T3; T1, 1 h before model establishment; T2, 1 h after model establishment; T3, on the 2nd weekend after injection; T4, on the 4th weekend after injection; MWT, mechanical withdrawal threshold; TWL, thermal withdrawal latency; DNP, diabetic neuropathic pain; TSN, tanshinone IIA; DRB, 5, 6-dichlorobenzimidazole1- β -D-ribofuranoside; PDTC, pyrrolidine dithiocarbamate.

Table 4 NCV at different time points in five groups.					
Parameter	Group	T1	T2	T3	T4
NCV (m/s)	Control $(n = 8)$ DNP $(n = 8)$ TSN $(n = 8)$ TSN + DRB $(n = 8)$ TSN + PDTC $(n = 8)$	$\textbf{33.87} \pm \textbf{2.12}$	$\begin{array}{c} 34.21 \pm 3.51 \\ 17.73 \pm 0.83 \% \\ 18.18 \pm 0.82 \% \\ 18.86 \pm 1.23 \% \\ 18.29 \pm 1.11 \% \end{array}$	$\begin{array}{c} \textbf{32.13} \pm \textbf{2.21} \\ \textbf{16.84} \pm \textbf{0.79*\%} \\ \textbf{22.23} \pm \textbf{1.01*} \# \% \\ \textbf{17.88} \pm \textbf{1.01*\%} \\ \textbf{17.33} \pm \textbf{0.95*\%} \end{array}$	34.40 ± 3.12 15.36 ± 0.47*% 27.61 ± 1.28*#%&\$ 16.52 ± 0.69*% 15.01 ± 0.79*%

Note: *, p < 0.05 compared with the control group at the same time point; $^{\sharp}$, p < 0.05 compared with the DNP group at the same time point; $^{\sharp}$, p < 0.05 compared with the time point of T1; $^{\sharp}$, p < 0.05 compared with the time point of T2; $^{\sharp}$, p < 0.05 compared with the time point of T3; T1, 1 h before model establishment; T2, 1 h after model establishment; T3, on the 2nd weekend after injection; T4, on the 4th weekend after injection; NCV, nerve conduction velocity; DNP, diabetic neuropathic pain; TSN, tanshinone IIA; DRB, 5, 6-dichlorobenzimidazole1- β -D-ribofuranoside; PDTC, pyrrolidine dithiocarbamate.

Structures of the sciatic nerve in the control, DNP, TSN, TSN + DRB and TSN + PDTC groups

The results of TEM (Fig. 1) implied that the myelinated nerve fibers of rats in the control group were clear and complete, and the microtubules in the axon were regularly arranged. In the DNP, TSN + DRB and TSN + PDTC groups, the axon of the myelinated nerve was atrophied and deformed, and the axon membrane was separated from the myelin sheath that was folded, thin or round along the axon. In the TSN group, the structure of nerve fibers slightly changed; the microfilaments and microtubules of mitochondrion were evenly arranged, and complete myelinated nerve fibers were observed. The fractures of myelin lamellae were small and focal, and the axon membrane had a clear structure and was tightly attached to the myelin sheath.

Distribution of the sciatic nerve in the control, DNP, TSN, TSN + DRB and TSN + PDTC groups

In the control and TSN groups, the myelinated nerve fibers of the sciatic nerve were distributed evenly, and each cell was plump with a uniform thickness of myelin sheath. However, in the DNP, TSN + DRB and TSN + PDTC groups, the myelinated nerve fibers of the sciatic nerve were distributed unevenly, the sciatic nerve shrank, and the diameter of the nerve decreased (Fig. 2).

Levels of antioxidase in the sciatic nerve among the control, DNP, TSN, TSN + DRB and TSN + PDTC groups

The antioxidase levels in the sciatic nerves among the five groups are shown in Table 5. Compared with the control group, the SOD and GSH-Px levels in the sciatic nerves decreased, while the MDA level increased in the other groups (all p < 0.05). Compared with the DNP group, the SOD and GSH-Px levels in the sciatic nerves increased, while the MDA level decreased in the TSN group (all p < 0.05). Compared with the TSN group, the TSN + DRB and TSN + PDTC groups had reduced SOD and GSH-Px levels in the sciatic nerves but increased MDA contents (all p < 0.05). No significant differences in the MDA, SOD and GSH-Px levels were found among the DNP, TSN + DRB and TSN + PDTC groups (all p > 0.05).

The mRNA and protein expression of Nrf2, HO-1, I κ B, Keap1 and NF- κ B in the control, DNP, TSN, TSN + DRB and TSN + PDTC groups

The mRNA and protein expression levels of Nrf2/ARE and NF- κ B signaling pathway-related genes (Nrf2, HO-1, I κ B, Keap1 and NF- κ B) are displayed in Fig. 3. Compared with the control group, the mRNA and protein expression levels of Nrf2, HO-1 and I κ B were reduced in the sciatic nerve of the DNP, TSN, TSN + DRB and TSN + PDTC groups.

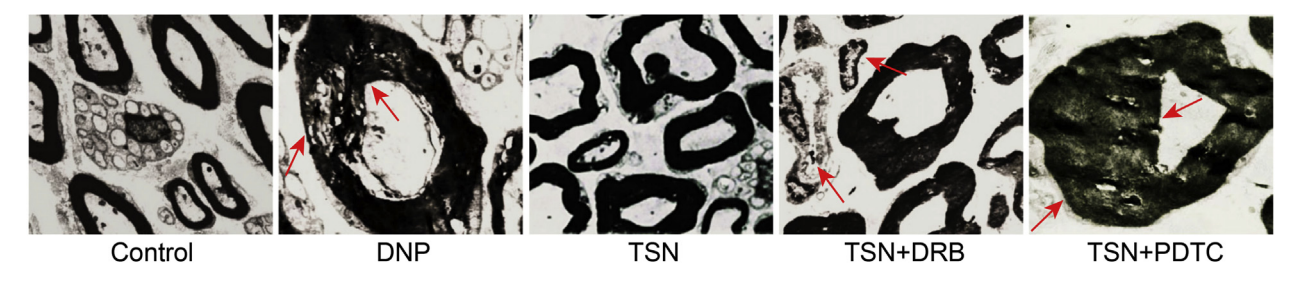


Figure 1. Microscopic examination of the structures of the sciatic nerve in axon cross sections among five groups (\times 11000). Note: the red arrows point to the changing sites of the myelinated nerve fibers of the sciatic nerve of rats; DNP, diabetic neuropathic pain; TSN, tanshinone IIA; DRB, 5,6-dichlorobenzimidazole1-β-D-ribofuranoside; PDTC, pyrrolidine dithiocarbamate.

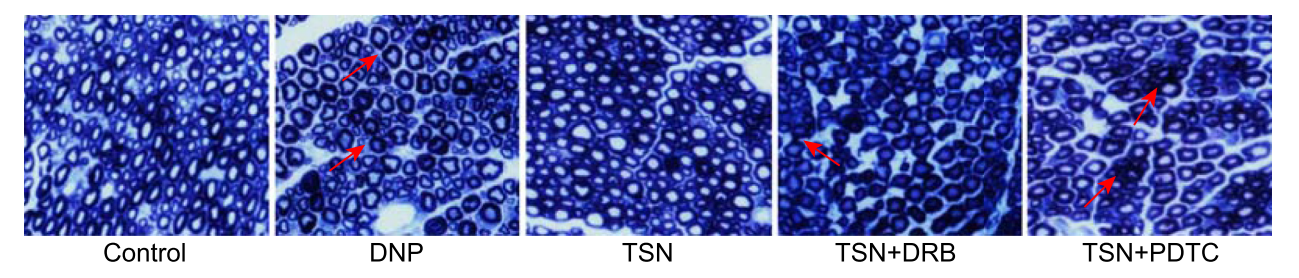


Figure 2. Toluidine blue staining for the density, form and thickness of the sciatic nerve among five groups (\times 400). Note: the red arrows point to the sciatic nerves that shrank; DNP, diabetic neuropathic pain; TSN, tanshinone IIA; DRB, 5,6-dichlorobenzimidazole1-β-p-ribofuranoside; PDTC, pyrrolidine dithiocarbamate.

Table 5 Levels of antioxidase in the sciatic nerves among five groups.						
Group	SOD (U/mg prot)	MDA (U/mgprot)	GSH-Px (U/mgprot)			
Control (n = 8)	39.53 ± 2.11	1.61 ± 0.11	36.41 ± 1.45			
DNP $(n = 8)$	$27.27 \pm 1.23*$	$\textbf{7.02}\pm\textbf{0.98*}$	$25.99 \pm 1.23*$			
TSN (n = 8)	33.01 \pm 1.89*#	4.23 \pm 0.31*#	31.02 \pm 1.67*#			
TSN + DRB (n = 8)	$27.32 \pm 1.27*$	$\textbf{6.94} \pm \textbf{0.19*}$	$25.45 \pm 1.11*$			
TSN + PDTC (n = 8)	27.11 ± 1.21*	$\textbf{6.89} \pm \textbf{0.12*}$	25.69 ± 1.33*			

Note: *, p < 0.05 compared with the control group at the same time point; ", p < 0.05 compared with the DNP group at the same time point; DNP, diabetic neuropathic pain; TSN, tanshinone IIA; DRB, 5, 6-dichlorobenzimidazole1- β -p-ribofuranoside; PDTC, pyrrolidine dithiocarbamate; SOD, superoxide dismutase; MDA, malondialdehyde; GSH-Px, erythrocyte glutathione peroxidase.

Furthermore, the mRNA and protein levels of Keap1 and NF- κ B were elevated in those groups (all p < 0.05). Compared with the DNP group, the TSN group had increased mRNA and protein expression of Nrf2, HO-1 and I κ B in the sciatic nerve but also had decreased mRNA and protein expression of Keap1 and NF- κ B (all p < 0.05). The mRNA and protein expression of Nrf2, HO-1 and I κ B in the sciatic nerve were decreased, while the levels of Keap1 and NF- κ B were higher in the TSN + DRB and TSN + PDTC groups than in the TSN group (all p < 0.05). There were no significant differences in the mRNA and protein expression of Nrf2, HO-1, I κ B, Keap1 and NF- κ B among the DNP, TSN + DRB and TSN + PDTC groups (all p > 0.05).

Discussion

Neuropathic pain is a serious disease that does harm to both the physical and mental health of many people worldwide [9]. Great efforts have been made to address this problem; for example, evidence-based guidelines for curing neuropathic pain were launched by the Neuropathic Pain Special Interest Group of the International Association for the Study of Pain. Unfortunately, we are still far away from providing adequate pain relief [21]. Notably, studies have indicated that TSN IIA alleviates neuropathic pain through a regulatory network [22]. Zhang et al. (2015) further demonstrated that Tan IIA is protective against Parkinson's disease via the regulation of Nrf2/ARE [23]. In addition, Tan IIA was confirmed to be a tumor suppressor in human breast cancer through attenuation of the NF-kB signaling pathway [24]. Hence, this study aimed to investigate the effects of TSN IIA on neuropathic pain via the Nrf2/ARE and NF-κB signaling pathways and to explore alternative therapies for neuropathic pain.

In this study, the NCV and behavioral tests showed that compared with the DNP group, the NCV, MWT and TWL in the TSN group were significantly increased, suggesting that TSN IIA could increase MWT, TWL and NCV and has protective effects on the sciatic nerve. A study revealed that TSN IIA alleviated neuropathic pain by suppressing the HMGB1-TLR4 pathway, which decreased pro-inflammatory cytokines and upregulated IL-10 [22]. Decreased NCV and sciatic nerve dysfunction were the main indicators of DNP, and NCV was an early and reliable index for DNP [25]. Shen et al. (2011) reported that TSN IIA had a proliferative effect on neuronal cells; specifically, TSN IIA enhanced neuron regeneration [26]. Moreover, the neuroprotective effect of TSN IIA has also been reported in diabetic rats [27]. It has been shown that TSN IIA could protect PC12 cells induced by serum deprivation against apoptosis [28]. Dong et al. (2009) demonstrated that TSN IIA has neuroprotective functions in permanent focal cerebral ischemia by restraining the oxidative stress and the inflammatory insult mediated by radicals [29]. In addition, the TSN group had decreased blood glucose and MDA and increased SOD and GSH-Px compared with the control group. Furthermore, the TSN + DRB and TSN + PDTC groups had increased blood glucose and MDA and decreased SOD and GSH-Px compared with the TSN group. All these findings indicated that TSN IIA is an antioxidant of the sciatic nerve, which could decrease blood glucose in rats with DNP. Consistently, treatment with TSN IIA lowered blood glucose levels in type 2 diabetes mellitus rats using STZ and a high-fat diet [30]. Furthermore. TSN IIA treatment decreased the MDA content and increased SOD activity in rats with hypertension-induced

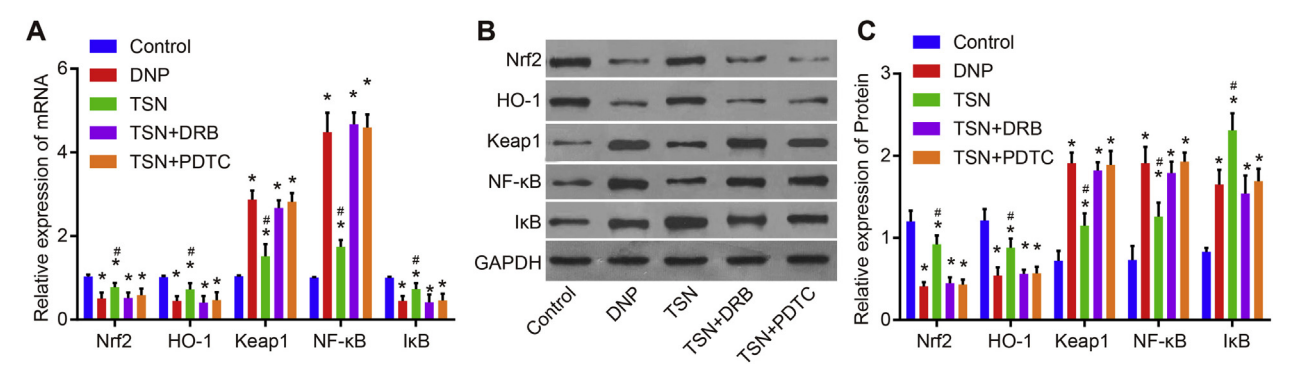


Figure 3. The mRNA and protein expression levels of Nrf2/ARE and NF- κ B signaling pathway-related genes (Nrf2, HO-1, I κ B, Keap1 and NF- κ B). Note: A, mRNA expression levels of Nrf2/ARE and NF- κ B signaling pathway-related genes determined by reverse transcription quantitative polymerase chain reaction; B, proteins of the Nrf2/ARE and NF- κ B signaling pathway-related genes as determined by western blot analysis; C, protein expression levels of the Nrf2/ARE and NF- κ B signaling pathway-related genes as determined by western blot analysis; *, P < 0.05 compared with the control group at the same time point; P < 0.05 compared with the DNP group at the same time point; DNP, diabetic neuropathic pain; TSN, tanshinone IIA; DRB, 5,6-dichlorobenzimidazole1- ρ -p-ribofuranoside; PDTC, pyrrolidine dithiocarbamate.

left ventricular hypertrophy [31]. Additionally, TSN IIA markedly reduced STZ-induced elevation in acetylcholinesterase (AChE) activity and the MDA level and significantly inhibited STZ-induced reduction in SOD and GSH-Px activities in the parietal cortex and hippocampus [32]. Taken together, these results show that TSN IIA is a promising therapy target for DNP due to its antioxidant and neuroprotective features.

Furthermore, in our study, in comparison to the DNP group, the mRNA and protein expression levels of Nrf2, HO-1 and IkB in the sciatic nerve of the TSN group significantly increased, while the levels of Keap1 and NF-κB significantly decreased. This suggested that TSN IIA promoted the expression of Nrf2/ARE signaling pathway-related genes (Nrf2, HO-1 and IκB) and inhibited the expression of NF-κB signaling pathway-related genes (Keap1 and NF-κB). Therefore, TSN IIA may attenuate DNP through its effect on the Nrf2/ARE and NF-κB signaling pathways. It has been demonstrated that pathways including hexosamine, polyol, advanced glycation-end-product (AGE) and protein kinase C (PKC) were involved in diabetic complications [33]. Previous experiments demonstrated that the activation of the Nrf2/ARE signaling pathway could contribute to neurological function in subarachnoid hemorrhage rats and prevent liver injuries [34]. The Nrf2 protein is translocated into the nucleus and forms a transcriptional complex with the musculo-aponeurotic fibrosarcoma family proteins, inducing neuroprotective genes regulated by Nrf2 [15]. Then, Nrf2 with Maf family proteins binds to the promoter region of a number of genes with the ARE regulatory sequence encoding antioxidase and phase 2 enzymes, such as HO-1, SOD, GSH-Px, and NAD(P)H [35]. NF-κB is activated by IkB when cells are under inflammatory conditions [36]. The inhibition of the NF-kB signaling pathway is also found to attenuate neuropathic pain symptoms and improve morphine analgesia in a rat model of neuropathy [37]. Wang et al. (2014) reported that TSN IIA activated the Nrf2 signaling pathway and upregulated the mRNA and protein expression of Nrf2 [38]. Guan et al. (2016) identified that TSN IIA could prevent acetaminophen-induced hepatotoxicity by increasing expression of Nrf2 target genes [39]. Bai et~al. (2016) found that through the suppression of the NF- κ B signaling pathway, TSN IIA could lead to the death of colon cancer cells [40]. In summary, it indicates that TSN IIA attenuates DNP by promoting the expression of Nrf2/ARE signaling pathway-related genes and inhibiting the expression of NF- κ B signaling pathway-related genes.

In conclusion, TSN IIA alleviates DNP via activation of the Nrf2/ARE signaling pathway and inhibition of the NF- κ B signaling pathway and may be an attractive candidate for the treatment of DNP in the future. However, since the experimental animals in this study are rats, whether TSN IIA has the same effect in larger animals or humans remains to be determined.

Funding

This work was supported by the Science and Technology Developmental Foundation of Hangzhou City (Grant No. 20170533B31).

Acknowledgements

We would like to thank our researchers for their hard work and reviewers for their valuable advice.

References

- Cohen SP, Mao J. Neuropathic pain: mechanisms and their clinical implications. BMJ 2014;348:f7656.
- [2] O'Connor AB. Neuropathic pain: quality-of-life impact, costs and cost effectiveness of therapy. Pharmacoeconomics 2009; 27:95—112.
- [3] Meng W, Deshmukh HA, van Zuydam NR, Liu Y, Donnelly LA, Zhou K, et al. A genome-wide association study suggests an

association of Chr8p21.3 (GFRA2) with diabetic neuropathic pain. Eur J Pain 2015;19:392—9.

- [4] Barrett AM, Lucero MA, Le T, Robinson RL, Dworkin RH, Chappell AS. Epidemiology, public health burden, and treatment of diabetic peripheral neuropathic pain: a review. Pain Med 2007;8(Suppl. 2):S50—62.
- [5] Gao F, Zheng ZM. Animal models of diabetic neuropathic pain. Exp Clin Endocrinol Diabetes 2014;122:100—6.
- [6] Wang S, Xu H, Zou L, Xie J, Wu H, Wu B, et al. LncRNA uc.48+ is involved in diabetic neuropathic pain mediated by the P2X3 receptor in the dorsal root ganglia. Purinergic Signal 2016;12: 139–48.
- [7] Kerstman E, Ahn S, Battu S, Tariq S, Grabois M. Neuropathic pain. Handb Clin Neurol 2013;110:175–87.
- [8] Schreiber AK, Nones CF, Reis RC, Chichorro JG, Cunha JM. Diabetic neuropathic pain: physiopathology and treatment. World J Diabetes 2015;6:432–44.
- [9] Tang J, Zhu C, Li ZH, Liu XY, Sun SK, Zhang T, et al. Inhibition of the spinal astrocytic JNK/MCP-1 pathway activation correlates with the analgesic effects of tanshinone IIA sulfonate in neuropathic pain. J Neuroinflammation 2015;12:57.
- [10] Sun D, Shen M, Li J, Li W, Zhang Y, Zhao L, et al. Cardioprotective effects of tanshinone IIA pretreatment via kinin B2 receptor-Akt-GSK-3beta dependent pathway in experimental diabetic cardiomyopathy. Cardiovasc Diabetol 2011;10:4.
- [11] Hao W, Chen L, Wu LF, Yang F, Niu JX, Kaye AD, et al. Tanshinone IIA exerts an antinociceptive effect in rats with cancer-induced bone pain. Pain Physician 2016;19:465—76.
- [12] Zhang HS, Wang SQ. Nrf2 is involved in the effect of tanshinone IIA on intracellular redox status in human aortic smooth muscle cells. Biochem Pharmacol 2007;73:1358–66.
- [13] Nioi P, McMahon M, Itoh K, Yamamoto M, Hayes JD. Identification of a novel Nrf2-regulated antioxidant response element (ARE) in the mouse NAD(P)H:quinone oxidoreductase 1 gene: reassessment of the ARE consensus sequence. Biochem J 2003; 374:337—48.
- [14] Kwak MK, Wakabayashi N, Greenlaw JL, Yamamoto M, Kensler TW. Antioxidants enhance mammalian proteasome expression through the Keap1-Nrf2 signaling pathway. Mol Cell Biol 2003;23:8786-94.
- [15] Neymotin A, Calingasan NY, Wille E, Naseri N, Petri S, Damiano M, et al. Neuroprotective effect of Nrf2/ARE activators, CDDO ethylamide and CDDO trifluoroethylamide, in a mouse model of amyotrophic lateral sclerosis. Free Radic Biol Med 2011;51:88–96.
- [16] Ren D, Ma W, Guo B, Wang S. Aloperine attenuates hydrogen peroxide-induced injury via anti-apoptotic activity and suppression of the nuclear factor-kappaB signaling pathway. Exp Ther Med 2017:13:315—20.
- [17] Liu Y, Su C, Shan Y, Yang S, Ma G. Targeting Notch1 inhibits invasion and angiogenesis of human breast cancer cells via inhibition nuclear factor-kappaB signaling. Am J Transl Res 2016;8:2681–92.
- [18] Jin UH, Suh SJ, Chang HW, Son JK, Lee SH, Son KH, et al. Tanshinone IIA from Salvia miltiorrhiza BUNGE inhibits human aortic smooth muscle cell migration and MMP-9 activity through AKT signaling pathway. J Cell Biochem 2008;104: 15-26
- [19] Rojewska E, Popiolek-Barczyk K, Kolosowska N, Piotrowska A, Zychowska M, Makuch W, et al. PD98059 influences immune factors and enhances opioid analgesia in model of neuropathy. PLoS One 2015:10:e0138583.
- [20] Morrow TJ. Animal models of painful diabetic neuropathy: the STZ rat model. Curr Protoc Neurosci 2004. https://doi.org/10. 1002/0471142301.ns0918s29. [Chapter 9]:Unit 9 18.

- [21] Dworkin RH, O'Connor AB, Audette J, Baron R, Gourlay GK, Haanpaa ML, et al. Recommendations for the pharmacological management of neuropathic pain: an overview and literature update. Mayo Clin Proc 2010;85:S3—14.
- [22] Ma YQ, Chen YR, Leng YF, Wu ZW. Tanshinone IIA down-regulates HMGB1 and TLR4 expression in a spinal nerve ligation model of neuropathic pain. Evid Based Complement Alternat Med 2014;2014;639563.
- [23] Zhang XS, Ha S, Wang XL, Shi YL, Duan SS, Li ZA. Tanshinone IIA protects dopaminergic neurons against 6-hydroxydopamine-induced neurotoxicity through miR-153/NF-E2-related factor 2/antioxidant response element signaling pathway. Neuroscience 2015;303:489–502.
- [24] Lin C, Wang L, Wang H, Yang L, Guo H, Wang X. Tanshinone IIA inhibits breast cancer stem cells growth in vitro and in vivo through attenuation of IL-6/STAT3/NF-kB signaling pathways. J Cell Biochem 2013;114:2061-70.
- [25] Coppey LJ, Davidson EP, Dunlap JA, Lund DD, Yorek MA. Slowing of motor nerve conduction velocity in streptozotocininduced diabetic rats is preceded by impaired vasodilation in arterioles that overlie the sciatic nerve. Int J Exp Diabetes Res 2000:1:131—43.
- [26] Shen JL, Chen YS, Lin JY, Tien YC, Peng WH, Kuo CH, et al. Neuron regeneration and proliferation effects of danshen and tanshinone IIA. Evid Based Complement Alternat Med 2011; 2011:378907.
- [27] Liu Y, Wang L, Li X, Lv C, Feng D, Luo Z. Tanshinone IIA improves impaired nerve functions in experimental diabetic rats. Biochem Biophys Res Commun 2010;399:49—54.
- [28] Ji ZN, Liu GQ. Inhibition of serum deprivation-induced PC12 cell apoptosis by tanshinone II A. Acta Pharmacol Sin 2001;22: 459—62.
- [29] Dong K, Xu W, Yang J, Qiao H, Wu L. Neuroprotective effects of Tanshinone IIA on permanent focal cerebral ischemia in mice. Phytother Res 2009;23:608–13.
- [30] Wei Y, Gao J, Qin L, Xu Y, Wang D, Shi H, et al. Tanshinone I alleviates insulin resistance in type 2 diabetes mellitus rats through IRS-1 pathway. Biomed Pharmacother 2017;93: 352-8
- [31] Pang H, Han B, Yu T, Peng Z. The complex regulation of tanshinone IIA in rats with hypertension-induced left ventricular hypertrophy. PLoS One 2014;9:e92216.
- [32] Liu C, Wu Y, Zha S, Liu M, Wang Y, Yang G, et al. Treatment effects of tanshinone IIA against intracerebroventricular streptozotocin induced memory deficits in mice. Brain Res 2016;1631:137—46.
- [33] Brownlee M. Biochemistry and molecular cell biology of diabetic complications. Nature 2001;414:813—20.
- [34] Jiang YM, Wang Y, Tan HS, Yu T, Fan XM, Chen P, et al. Schisandrol B protects against acetaminophen-induced acute hepatotoxicity in mice via activation of the NRF2/ARE signaling pathway. Acta Pharmacol Sin 2016;37:382—9.
- [35] Wang AL, Niu Q, Shi N, Wang J, Jia XF, Lian HF, et al. Glutamine ameliorates intestinal ischemia-reperfusion Injury in rats by activating the Nrf2/Are signaling pathway. Int J Clin Exp Pathol 2015;8:7896–904.
- [36] Park JY, Moon JY, Park SD, Park WH, Kim H, Kim JE. Fruits extracts of Hovenia dulcis Thunb. suppresses lipopolysaccharidestimulated inflammatory responses through nuclear factor-kappaB pathway in Raw 264.7 cells. Asian Pac J Trop Med 2016;9:357–65.
- [37] Popiolek-Barczyk K, Makuch W, Rojewska E, Pilat D, Mika J. Inhibition of intracellular signaling pathways NF-kappaB and MEK1/2 attenuates neuropathic pain development and enhances morphine analgesia. Pharmacol Rep 2014;66:845–51.

- [38] Wang L, Zhang C, Guo Y, Su ZY, Yang Y, Shu L, et al. Blocking of JB6 cell transformation by tanshinone IIA: epigenetic reactivation of Nrf2 antioxidative stress pathway. AAPS J 2014;16:1214–25.
- Nrf2 antioxidative stress pathway. AAPS J 2014;16:1214—25.
 [39] Wang W, Guan C, Sun X, Zhao Z, Li J, Fu X, et al. Tanshinone IIA protects against acetaminophen-induced hepatotoxicity
- via activating the Nrf2 pathway. Phytomedicine 2016;23: 589-96.
- [40] Bai Y, Zhang L, Fang X, Yang Y. Tanshinone IIA enhances chemosensitivity of colon cancer cells by suppressing nuclear factor-kappaB. Exp Ther Med 2016;11:1085–9.